Supplementary Information

The Cross-Linked Polymer-Derived B/N co-Doped Carbon Materials with Selective Capture of CO_2

Wuxue Zhao,[a] Sheng Han,[b] Xiaodong Zhuang,*[a] Fan Zhang,*[a] Yiyong Mai[a] and Xinliang Feng[ac]

[a]School of Chemistry and Chemical Engineering, Shanghai Jiao Tong University, Shanghai 200240, China

[b]School of Chemical and Environmental Engineering, Shanghai Institute of Technology, Haiquan Road 100, 201418, Shanghai, P. R. China

[c]Center for Advancing Electronics Dresden & Department of Chemistry and Food Chemistry, Technische Universitaet Dresden, 01062 Dresden, Germany

E-mail address: fan-zhang@sjtu.edu.cn; zhuang@sjtu.edu.cn.

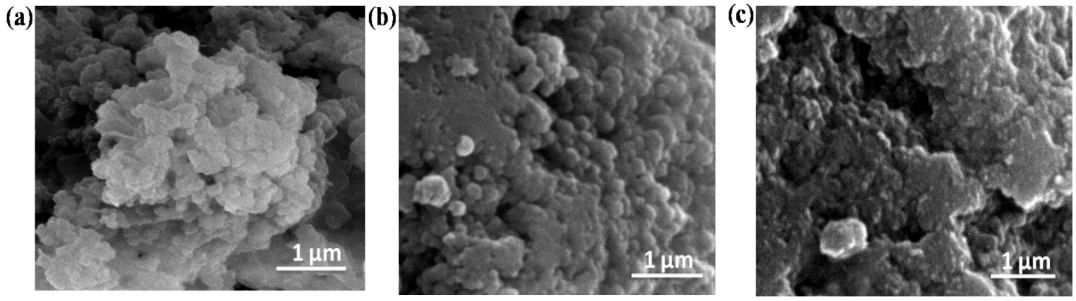

Figure. S1 SEM images of (a) PPs-BN-1, (b) PPs-BN-2 and (c) PPs-BN-3. The samples are homogeneous, composing of loose agglomerates of tiny particles with rough surface and irregular shape.

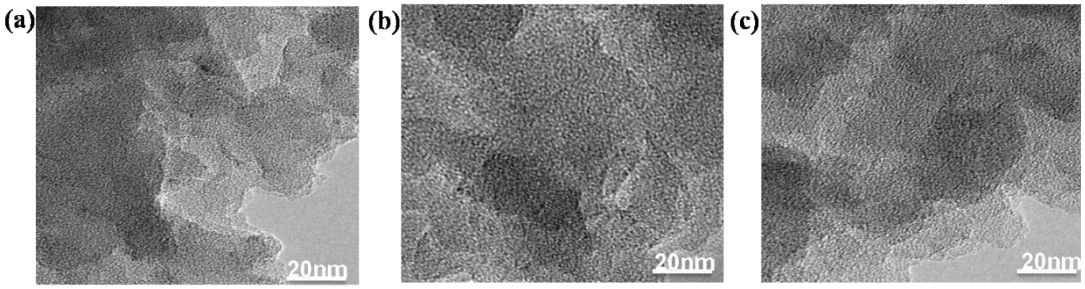

Figure. S2 TEM images of (a) PPs-BN-1, (b) PPs-BN-2 and (c) PPs-BN-3. The TEM images for both networks showed typical irregular structures as usually found for porous polymers.

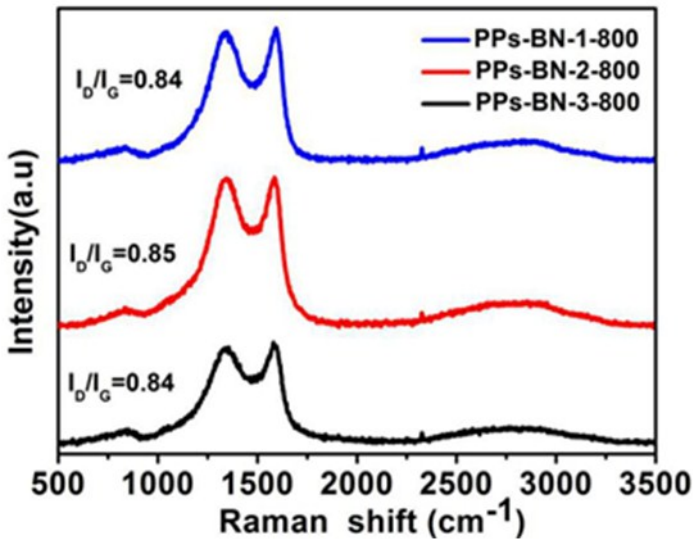

Figure. S3 Raman spectra of PPs-BN-i-800 (i=1, 2, 3).

Raman spectroscopy has been widely used to characterize the structure of carbon materials. The Raman spectra of PPs-BN-i-800 (i=1, 2, 3) were shown in Figure S3.

There are two prominent peaks at 1338.4 and 1593.5 cm^{-1}, corresponding to the D and G bands, respectively. The ID/IG ratio of PPs-BN-i-800 (i=1, 2, 3) (0.84-0.85) indicates that the presence of a certain graphitization degree for carbon materials after pyrolysis at 800 °C.

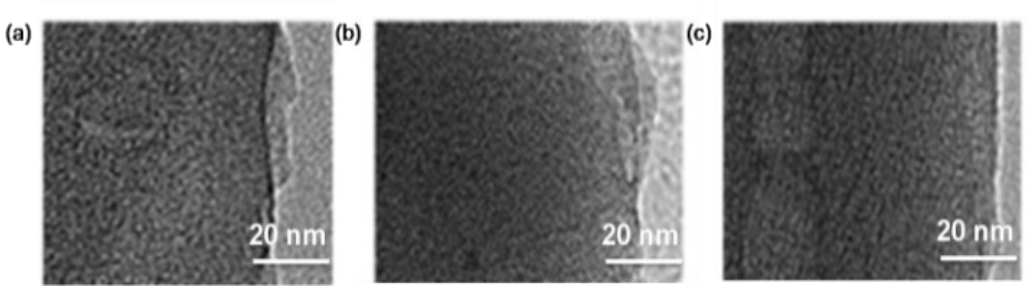

Figure. S4 TEM images of (a) PPs-BN-1-800. (b) PPs-BN-2-800 and (c) PPs-BN-3-800.

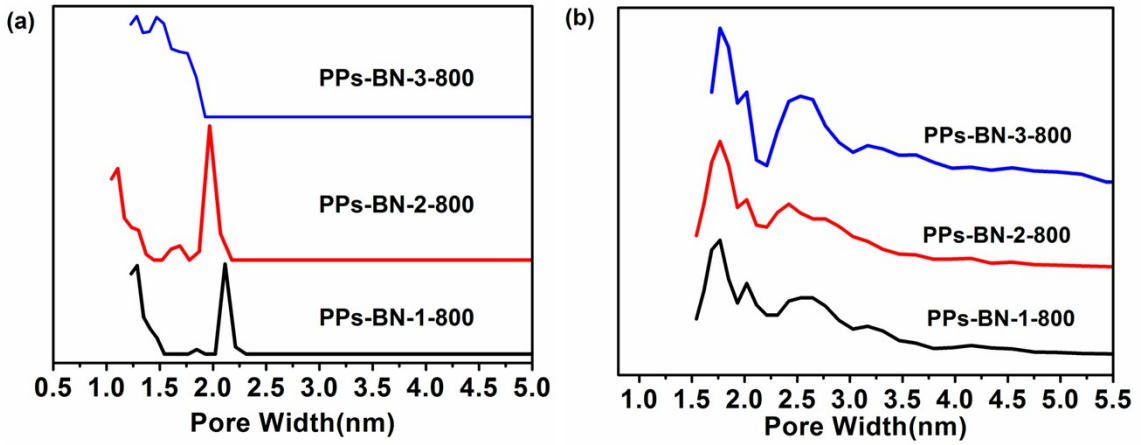

Figure. S5 Pore size distribution curves for PPs-BN-i-800 as calculated by NL-DFT from (a) N_2 (77 K) and (b) CO_2 (273 K) adsorption isotherms.

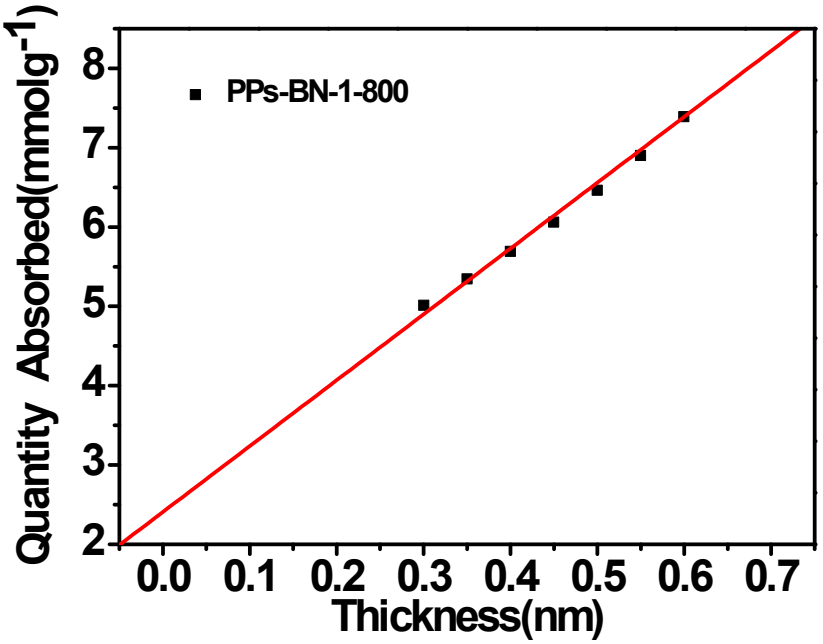
PPs-BN-1-800
Quantity Absorbed(mmolg-1)
Thickness(nm)
2
3
4
5
6
7
8
0.0
0.1
0.2
0.3
0.4
0.5
0.6
0.7

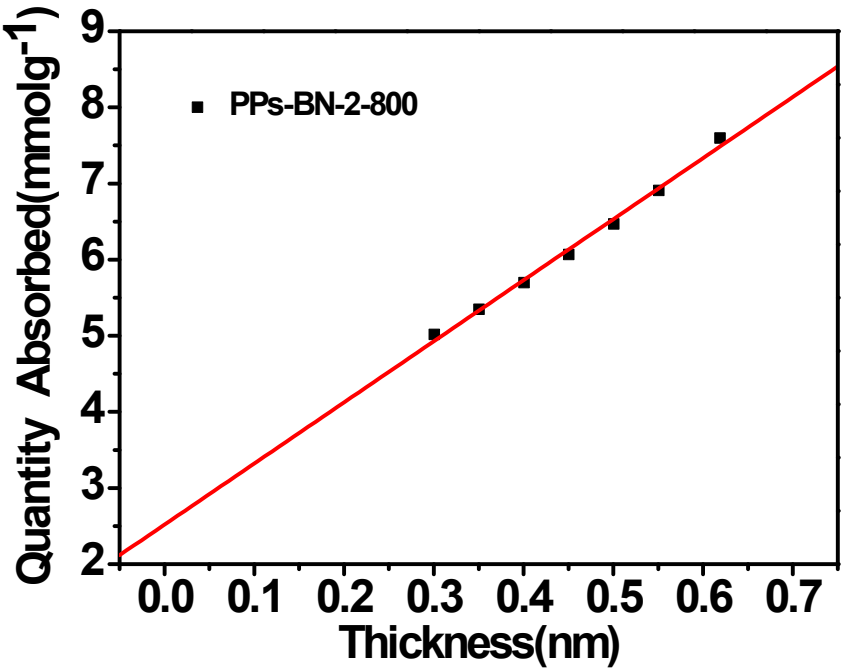
PPs-BN-2-800
Quantity Absorbed(mmolg-1)
Thickness(nm)
2
3
4
5
6
7
8
9
0.0
0.1
0.2
0.3
0.4
0.5
0.6
0.7

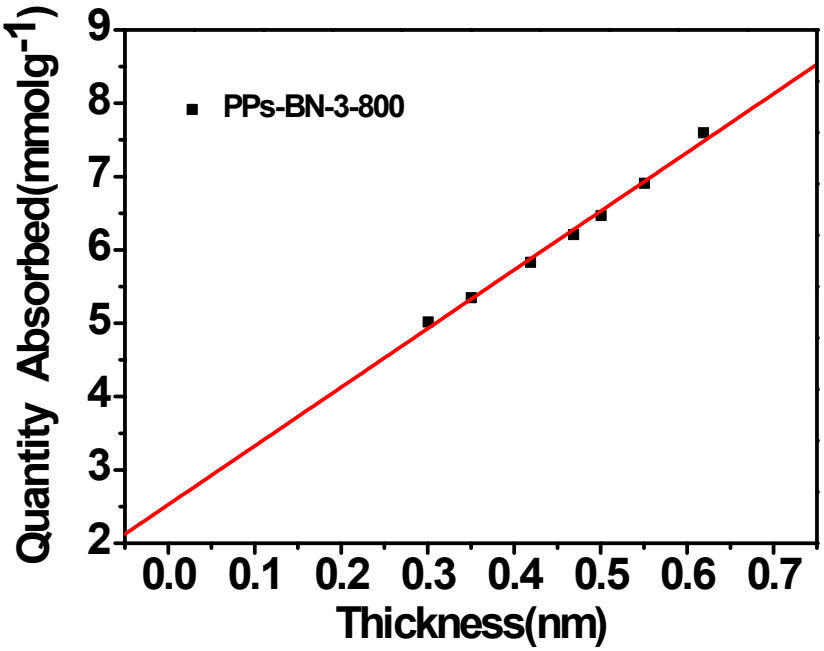

Figure. S6 BET specific surface area plot of PPs-BN-i-800 (i=1, 2, 3).

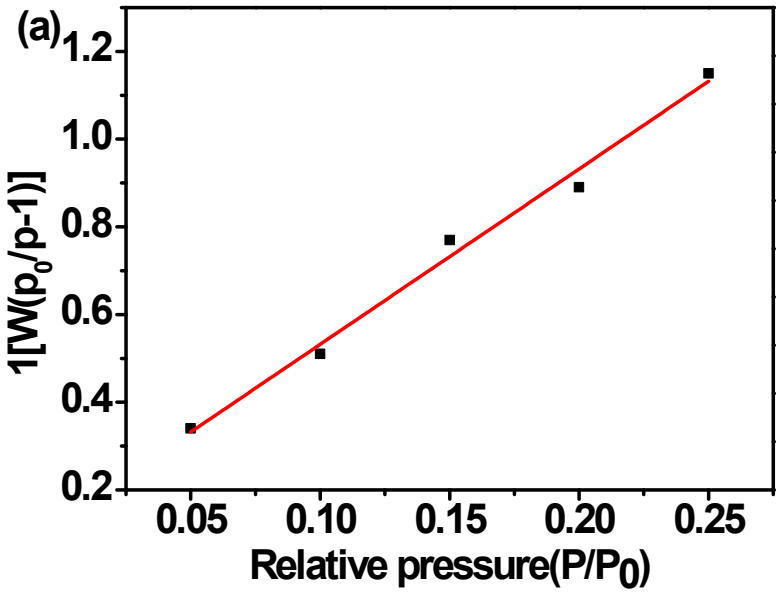

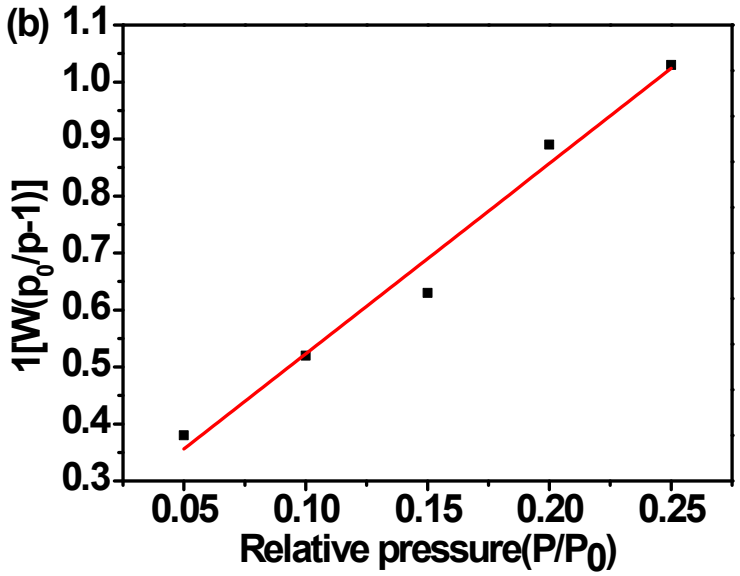

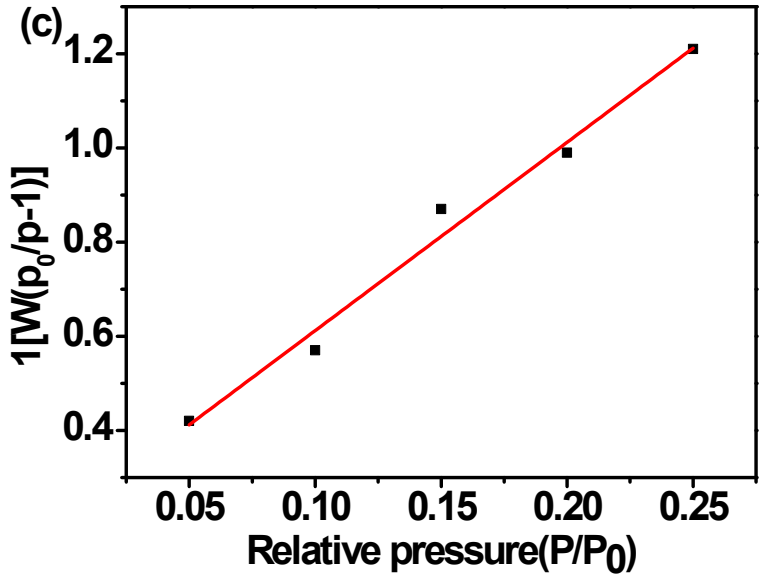

Figure. S7 The curve of the BET linear correlation (a) PPs-BN-1, (b) PPs-BN-2 and (c) PPs-BN-3.

Table S1. Physical properties for polymer networks and porous carbon and comparison of CO_2 uptake for various porous carbon at 273 K or 298 K and 1 bar.

Sample	N[a] [wt%]	S_{BET}[b] [$m^2 g^{-1}$]	CO_2 uptake [mmol g^{-1}]		CH_4 uptake [mmol g^{-1}]		Ref
			273 K	298 K	273 K	298 K	
PPs-BN-1-800	5.63	215	3.23	2.31	0.98	0.46	
PPs-BN-2-800	5.72	291	3.25	2.40	1.10	0.59	This work
PPs-BN-3-800	4.89	268	3.11	2.34	1.15	0.54	
MFB-600	1.74	490	-	2.25			Ref[1]
NC-800	3.0	263	2.65	1.95			Ref[2]
CP-4-800	0.47	3450	-	2.60			Ref[3]
3C-650N	2.95	741	-	2.43			Ref[4]
C600	20.2	362	-	1.90			Ref[5]
AC-800-2	/	2994	-	2.51			Ref[6]
FCDTPA-700	4.71	417	2.92				Ref[7]

[a] Derived from XPS analysis, [b] Surface area calculated from the N_2 adsorption isotherm using the BET method.

Table S2. The peak position and percentage for each N peak of porous carbon from XPS.

Sample	-N-B-		pyridinic-N		-N-C-		pyrrolic-N		graphitic-N	
	eV	%	eV	%	eV	%	eV	%	eV	%
PPs-BN-1-800	398.2	15.1	398.8	22.1	399.8	24.3	400.8	23.2	401.6	15.3
PPs-BN-2-800	397.8	21.9	398.5	19.8	399.6	21.1	401.0	20.1	401.8	17.1
PPs-BN-3-800	398.1	12.7	398.8	22.1	399.7	23.6	400.8	22.5	401.6	19.1

Virial graph for the adsorption of CO_2 at different temperature

The Virial equation can be written in the following form:[8]

$$\ln(n/P)=A_0+A_1n+A_2 \bullet\bullet n^2+A_3 \bullet\bullet n^3+\ldots$$

Where n is the amount adsorbed at pressure p and the first Virial coefficient, A_0 is a constant related to the Henry's law constant. In the low pressure range, the higher terms (A_2, A_3… etc) in the Virial equation could be ignored at low surface coverage. As shown in the plots, the term ln(n/P) shows the nearly linear relationship with adsorption amounts (as shown in Fig. S7-9 for CO_2).Therefore, the values of the first Virial coefficient (A_0) and the second Virial coefficient (A_1) which reflect the adsorbate-adsorbent interaction and adsorbate-adsorbate interactions, respectively, can be obtained from the linear fit of ln(n/P) versus n.

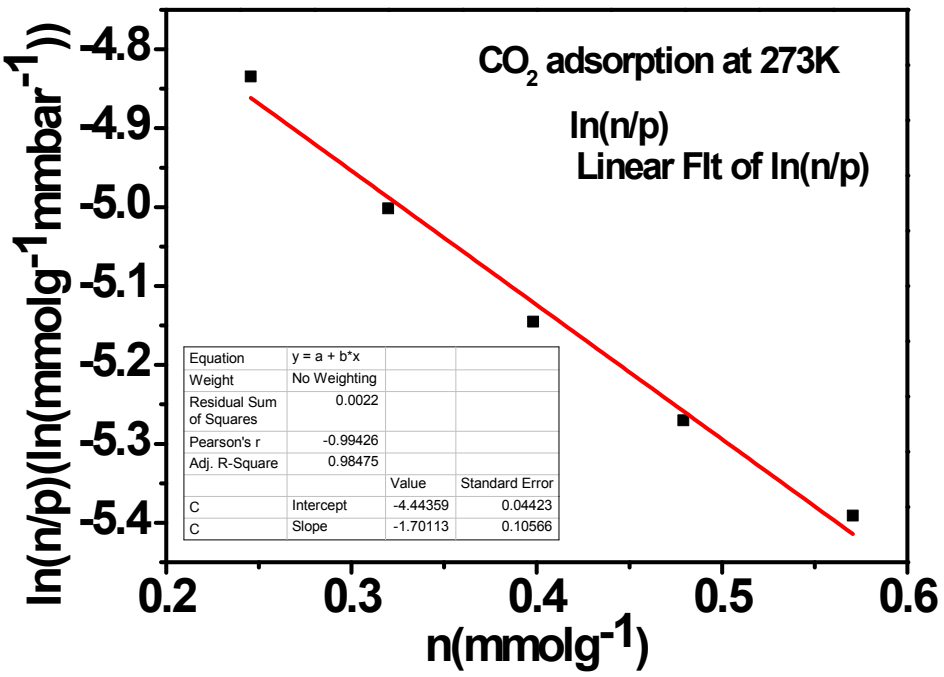

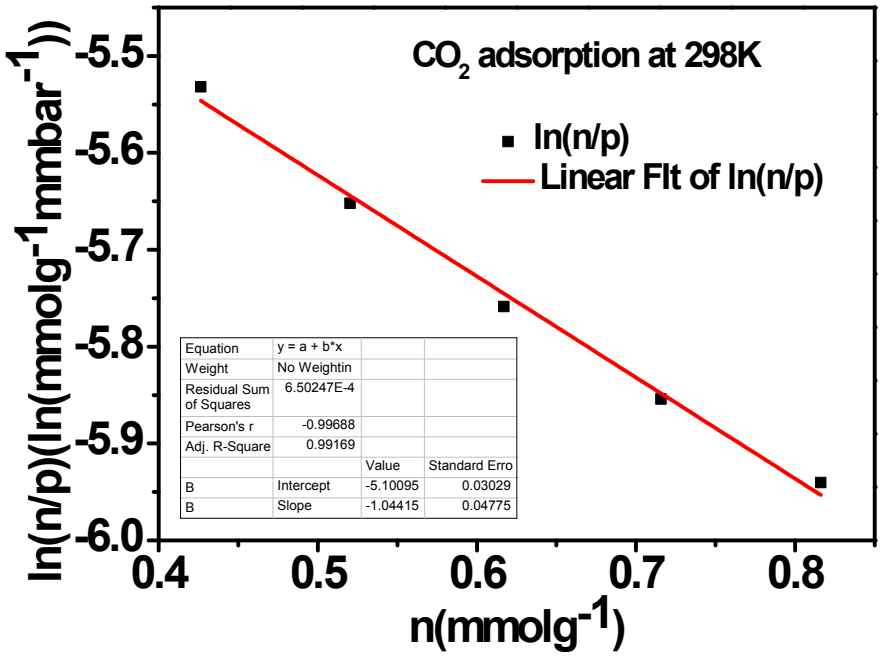

Figure. S8 Virial graph for the adsorption of CO_2 on PPs-BN-1-800 at 273 K and 298 K.

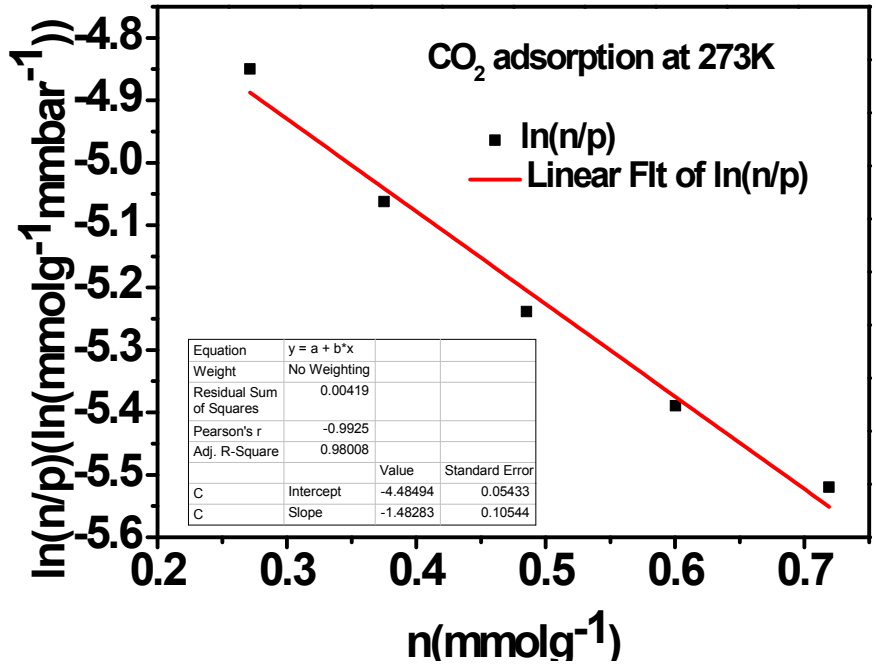

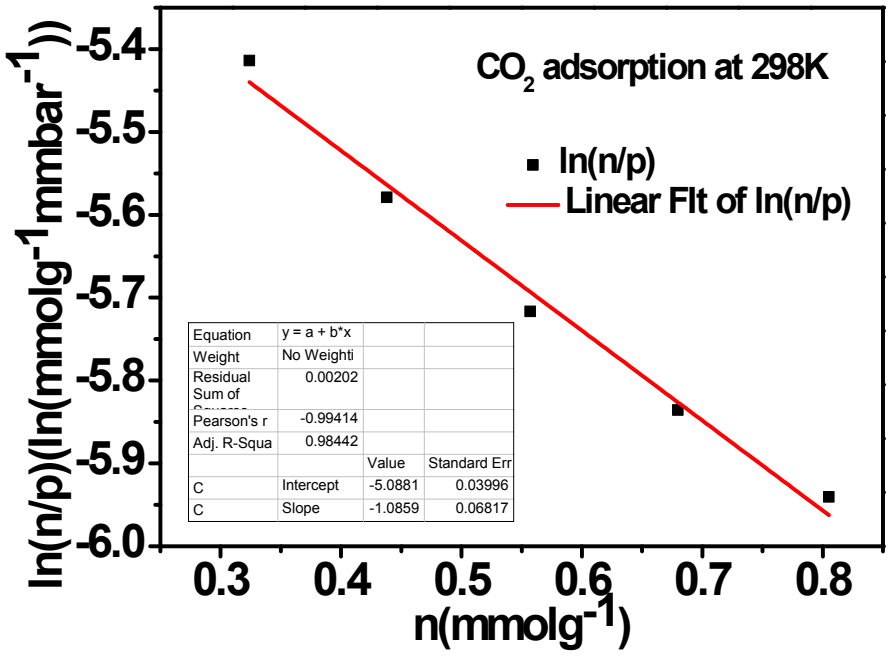

Figure. S9 Virial graph for the adsorption of CO_2 on PPs-BN-2-800 at 273 K and 298 K.

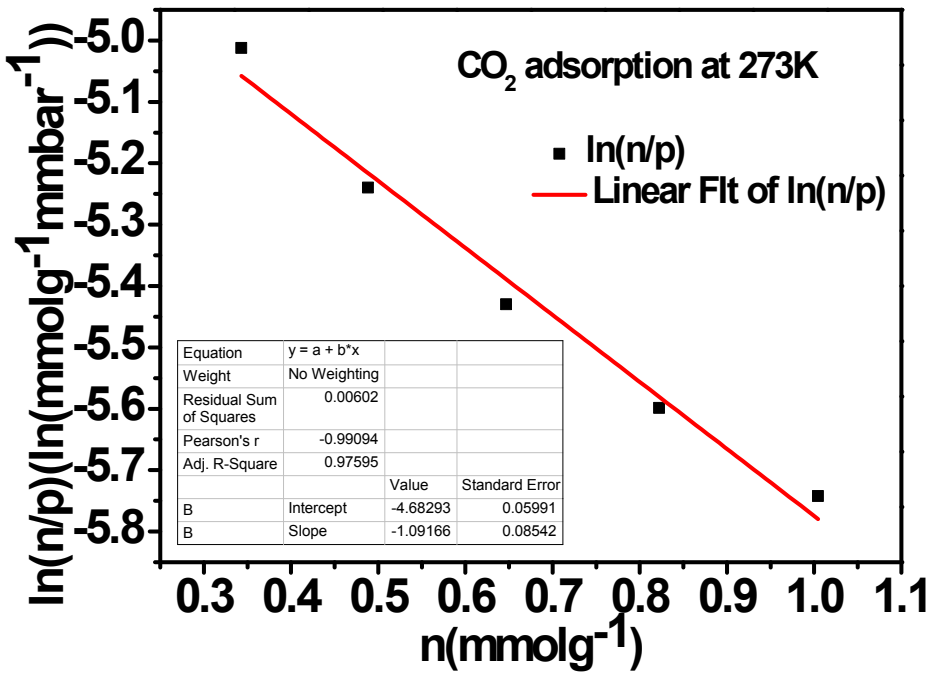

Equation	y = a + b*x		
Weight	No Weighting		
Residual Sum of Squares	0.00602		
Pearson's r	-0.99094		
Adj. R-Square	0.97595		
		Value	Standard Error
B	Intercept	-4.68293	0.05991
B	Slope	-1.09166	0.08542

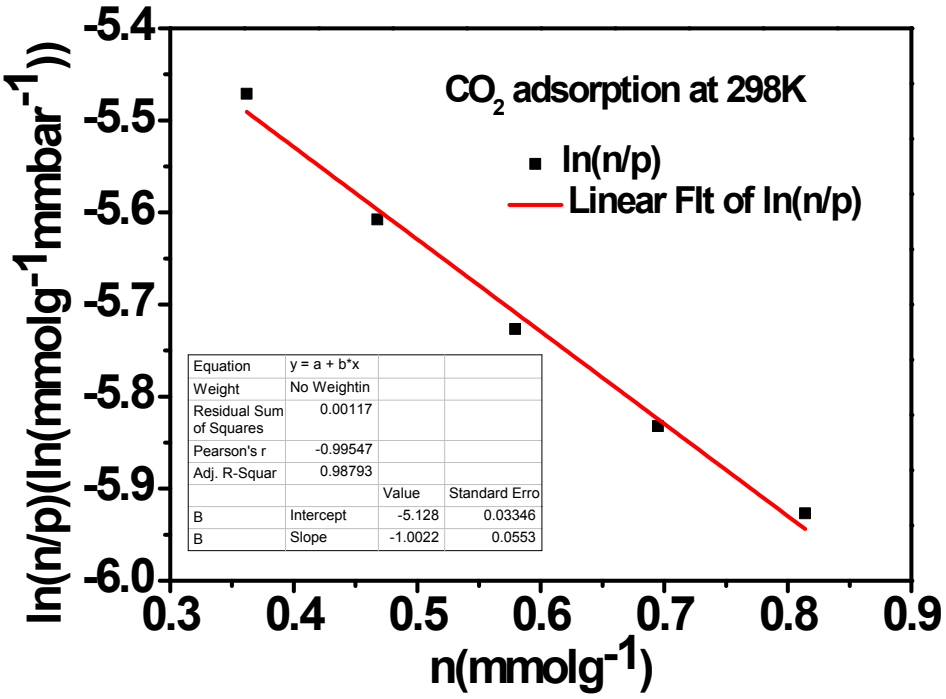

Equation	y = a + b*x		
Weight	No Weightin		
Residual Sum of Squares	0.00117		
Pearson's r	-0.99547		
Adj. R-Squar	0.98793		
		Value	Standard Erro
B	Intercept	-5.128	0.03346
B	Slope	-1.0022	0.0553

Figure. S10 Virial graph for the adsorption of CO_2 on PPs-BN-3-800 at 273 K and 298 K.

References

1. C. Pevida, T. C. Drage and C. E. Snape, *Carbon*, 2008, **46**, 1464.

2. M. Sevilla, J. B. Parra and A. B. Fuertes, *ACS appl.mater.inter.*, 2013, **5**, 6360.

3. M. Sevilla, P. Valle-Vigón and A. B. Fuertes, *Adv. Funct. Mater.,* 2011, **21**, 2781.

4. L. Liu, Q.-F. Deng, T.-Y. Ma, X.-Z. Lin, X.-X. Hou, Y.-P. Liu and Z.-Y. Yuan, *J. Mater. Chem.,* 2011, **21**, 16001.

5. F. Bai, Y. Xia, B. Chen, H. Su and Y. Zhu, *Carbon*, 2014, **79**, 213.

6. Z. Zhang, J. Zhou, W. Xing, Q. Xue, Z. Yan, S. Zhuo and S. Z. Qiao, *Phys. Chem. Chem. Phys.,* 2013, **15**, 2523.

7 X. Yang, M. Yu, Y. Zhao, C. Zhang, X. Wang and J.-X. Jiang, *J. Mater. Chem A*., 2014, **2**, 15139.

8. H. Xu, Y. B. He, Z. J. Zhang, S. C. Xiang, J. F. Cai, Y. J. Cui, Y. Yang, G. D. Qian and B. L. Chen. *J. Mater. Chem A,* 2013,**1**, 77.